Mining, Metallurgy & Exploration (2022) 39:1465–1473
https://doi.org/10.1007/s42461-022-00635-8

Rockmass Permeability Induced by Longwall Mining Under Deep Cover: Potential Gas Inflow from a Sheared Gas Well

Zoheir Khademian[1] · Kayode M. Ajayi[1] · Steven J. Schatzel[1] · Gabriel S. Esterhuizen[2] · Bo H. Kim[3]

Received: 14 February 2022 / Accepted: 2 June 2022 / Published online: 19 June 2022

Abstract
The stability of shale gas wells drilled through current and future coal reserves can be compromised by ground deformations due to nearby longwall mining. Depending on the longwall-induced rockmass permeability, the high-pressure explosive gas from the damaged well may reach mine workings and overwhelm the mine ventilation systems. This study uses geomechanical models to estimate the rockmass permeability induced by mining. A two-panel longwall model of a deep, 341-m-cover mining site in southwestern Pennsylvania is constructed in 3DEC to explicitly model the rockmass by a discrete fracture network (DFN) technique. Stress-induced fracture apertures and permeabilities are calculated across the model and are validated against permeability measurements. A fracture flow code (FFC) is developed to use these results to predict potential inflow to the mine should a gas well breach occur. One hundred DFN realizations are simulated, and the results show that for a gas pressure of 2.4 MPa, the average of the predicted inflow rates to this deep-cover mine is 0.006 m^3/s, significantly lower than the average inflow of 0.22 m^3/s for a shallow-cover mine (145-m deep) studied in the previous work (Khademian, et al. 2021). The result can help assess the potential hazards of a shale gas well breach for mine safety and evaluate the ventilation requirements to mitigate the risk.

1 Introduction

In the Northern Appalachian Basin of the USA, most of the production wells in shale gas reservoirs intersect with a bedded sequence of minable coal layers [7]. Active or future longwall operations can coexist with the shale gas production but require specific design considerations for ensuring the safety of both operations. In this situation, the gas wells are often positioned in the coal mine abutment pillars for protection of the well from the ground movement. One of the main safety hazards can be due to the longwall-induced stresses leading to excessive deformation and rupture in the gas well casing, compromising its integrity. Depending on the surrounding rock permeability, the potentially explosive, high-pressure gas from the hypothetical breach area may reach the mining area. Therefore, quantitative analyses of the potential gas inflow need an understanding of the rockmass permeability that can be changed by the mining-induced stress and subsurface movement.

In previous work [4], a geomechanical modeling methodology was developed based on the DFN technique for calculating the permeability evolution during mining of a shallow, 145-m-cover mine in Pittsburgh coal seam. In situ measurements were used for constraining and calibrating the range of DFN parameters in the model. The calibrated parameters, such as the initial aperture, density (total fracture area in unit volume of rock), and frictional properties of the DFNs, were used to construct a stochastic flow model. The results of 100 realizations showed that the average gas inflow rate to the mine was 0.22 m^3/s for a hypothetical gas well breach at the Sewickley coal bed horizon, 23 m above the mined coal seam. The weak Sewickley coal horizon indicates potential planes of weakness where longwall-induced horizontal displacement may damage gas well casing (Zhang, Dougherty, et al. 2020). This paper adopts the calibrated parameters and employs the same methodologies for calculating the permeability of a deeper mine, 341-m-cover site in the Pittsburgh seam. The modeling results are compared with the field measurement and then are used to calculate the potential

✉ Zoheir Khademian
opv9@cdc.gov

1 Pittsburgh Mining Research Division, CDC NIOSH, Pittsburgh, PA, USA

2 Independent Mining Engineer, Pittsburgh, PA, USA

3 CDC NIOSH, Spokane Mining Research Division, Spokane, WA, USA

gas volume flow rate to the mine in the case of a hypothetical, well-casing breach at the Sewickley horizon 32 m above the mine roof.

2 Methodology

A three-dimensional distinct element code, 3DEC, is used for constructing a pseudo-2D longwall model, i.e., the model dimension in the out-of-plane direction is 1 m. The DFN technique is used for explicitly modeling fractures in rockmass since fracture permeabilities vastly dominate the permeability associated with rock pores. This study adopts the methodology and calibrated parameters from previous work [4] and constructs the geomechanical model of a 341-m-deep longwall mine in the Pittsburgh coal bed. In situ permeability measurements are conducted and are used to check the modeling results. Finally, fracture apertures obtained from the calibrated geomechanical model are exported to FFC for estimating the possible range of gas flow to the mining area in the case of a breached gas well.

3 Description of mine site and in situ measurements

A longwall mine under 341 m of cover in southwestern Pennsylvania in the Pittsburgh coal bed is selected for this study. The proximity of Pittsburgh coal bed mines to the Marcellus shale formation has led to a geological condition where desirable energy resources overlie one another. The Marcellus shale and Pittsburgh coal seam share much of the same areas within Pennsylvania and West Virginia although they are 1200–2100 m apart in the strata. The selected mine site is located in a position overlying the Marcellus shale formation so that for shale gas production, gas wells may intersect with the longwall workings. The longwall panel is 456-m wide with a mining height of 2.3 m. The potential location of the gas well is within a 36.2-m by 80.3-m abutment pillar that is a part of a three-entry gateroad system between the first and second panels in the district. Overburden geology to the mining depth of 341 m was interpreted by correlating a test site gamma log and a nearby core hole [11]. The Pittsburgh coal seam is within the Monongahela group of the Pittsburgh formation that contains other major units such as the Sewickley coal. The weak Sewickley coal horizon at 308 m indicates potential planes of weakness that can be significantly affected by the longwall-induced deformation (Zhang, Dougherty, et al. 2020). The rock types in the overburden are shale, sandstone, sandy shale, limestone, coal, and shaley limestone with the field-scale geomechanical properties listed in Table 1 (Zhang, Su, et al. 2020).

Table 1 Geomechanical properties applied to the model for each lithology

Rock type	*E*	*ν*	*C*	*φ*°	*T*
Coal	2.1	0.3	1.9	28	0.3
Shale	11.6	0.25	11.7	35	4.5
Sandy shale	11.6	0.25	11.7	35	4.5
Sandstone	11.6	0.22	17.9	35	6.9
Limestone	17.4	0.25	15.9	35	6.1

E elastic modulus (GPa), *ν* Poisson's ratio, *C* cohesion (MPa), *φ* internal friction angle, *T* tensile strength (MPa)

Two monitoring boreholes were drilled in the overburden for conducting slug permeability tests as the first and second panels were mined nearby the test site. Due to the presence of standing water in the boreholes, falling head slug tests were conducted by the research team at regular intervals. The basis of the measurements is to use hydrologic methods to determine changing water head in boreholes using downhole piezometers over a portion of the mining life of the study panels.

Pre-mining permeability values were measured at a depth of 295 m at borehole A for a Gob Vent Borehole (GVB) location about 98 m away from the tailgate gateroad before mining the first panel (Fig. 1). These measurements show permeability ranges from 245 to 285 millidarcy (mD) at this location.

Borehole B was drilled around the center of the first panel (Fig. 1). The slug test was also performed at borehole B for post-mining permeability determinations at the depth of 265 m at the Uniontown coal horizon, over 300 m behind the active face. Permeability values ranged from 67 to 123 mD at this location.

4 Geomechanical model

3DEC is used for constructing a pseudo-2D longwall model of the study site (Fig. 1) with 1-m length in the out-of-plane direction. DFN is used for explicitly modeling fractures in rockmass since the fluid flow through fractures vastly dominates the flow through rock internal pores. This is mainly because the cross-sectional area of the fracture, and thus the flow rate through fractures, is several orders of magnitude larger than that of pores within the rock matrix.

4.1 Model geometry

From the core log data, 105 geologic layers were modeled each with a thickness greater than 0.6 m (Fig. 1). The model length is extended in the x direction to a total of 9000 m to avoid any boundary effects. One of the challenges in DFN

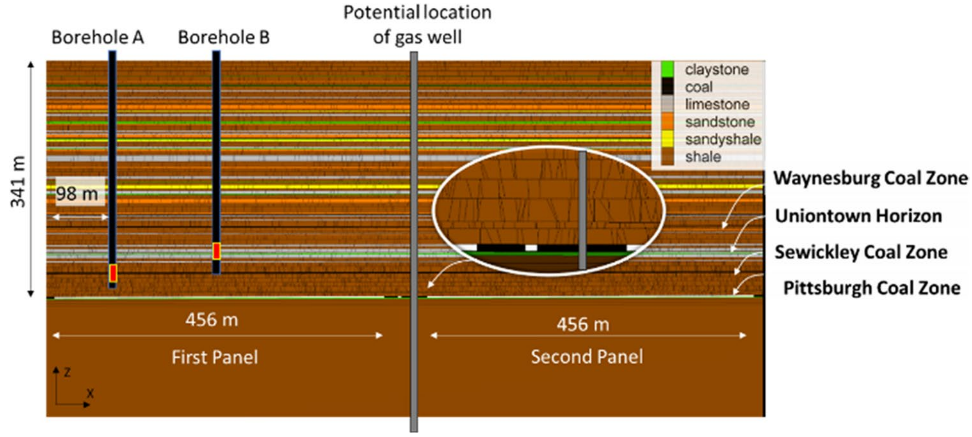

Fig. 1 Details of the central part of the 3DEC model of the deep longwall mine with DFN elements defining rockmass structures in 105 modeled lithologies. Boreholes A and B and their permeability test intervals are shown along with the potential location of a gas well in the abutment pillar

implementation for simulating fractured rock is how to constrain site-specific fracture geometries and frictional properties that best represent rockmass behaviors under stress. Fracture geometry is defined as the distribution of fracture orientation, length, and density. Observation from longwall-induced fracture orientations at longwall face suggests propagation of subvertical fractures perpendicular to the mining face [11]. Thus, the DFNs are modeled with a strike direction perpendicular to the face and a dip angle with a mean of 90 degrees. From field observations in Southwest Pennsylvania [5], the variation of the subvertical fracture dip angles is approximated to be 15° from 0–10 m above the mine roof, 12° from 10–30 m, 10° from 30–60 m, and 5° degree for the rest of the domain. Figure 2 shows the fracture dip and dip directions on a lower hemisphere stereonet by the fracture poles.

The length of fractures is assumed limited to the thickness of host strata with a negative power law distribution with a scaling exponent of 1.1. Uniform distribution is used for the fracture position within each individual lithology because fracture systems are mostly affected by the physical properties of the host rock (Feng 2018).

The fracture density is defined as the P_{32} value, which is the cumulated fracture surface in the specified region per unit volume. No data is available for the fracture density in this mining site, so the values are inferred from the previous calibration study on a shallow Pittsburgh coal longwall site [4]. Figure 3 shows the fracture densities applied to the model at different depths. Fracture densities are limited to a 0.1–0.3 m^2/m^3 range with higher densities applied to weaker zones that are defined by the logging data and field observations. The weak zones include the shallow weathered zone, Waynesburg horizon, Uniontown horizon, Sewickley horizon, and an interconnected longwall-induced fracture zone. The combined thickness of the caved area and the lower part of the fractured zone above it is defined as the interconnected fracture zone that represents a system of channels allowing flow transport

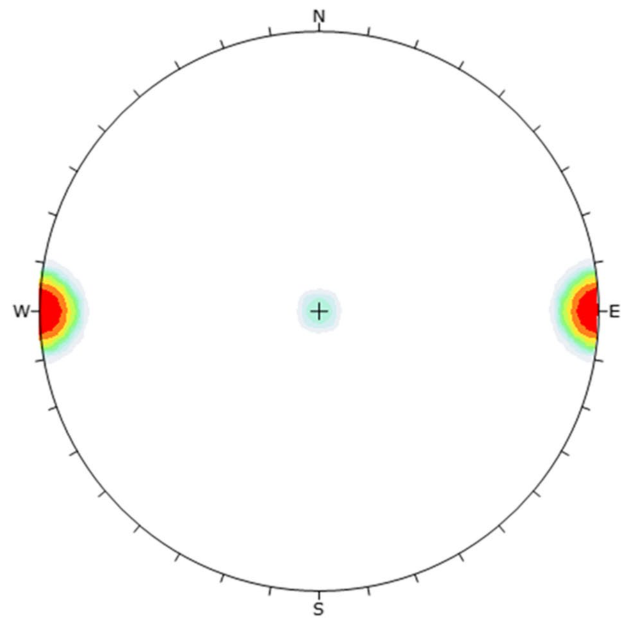

Color	Density Concentrations
	0.00 - 7.30
	7.30 - 14.60
	14.60 - 21.90
	21.90 - 29.20
	29.20 - 36.50
	36.50 - 43.80
	43.80 - 51.10
	51.10 - 58.40
	58.40 - 65.70
	65.70 - 73.00
Contour Data	Pole Vectors
Maximum Density	72.82%
Contour Distribution	Fisher
Counting Circle Size	1.0%

Fig. 2 Lower hemisphere stereonet of pole vectors of subvertical fractures and bedding planes in 3DEC model

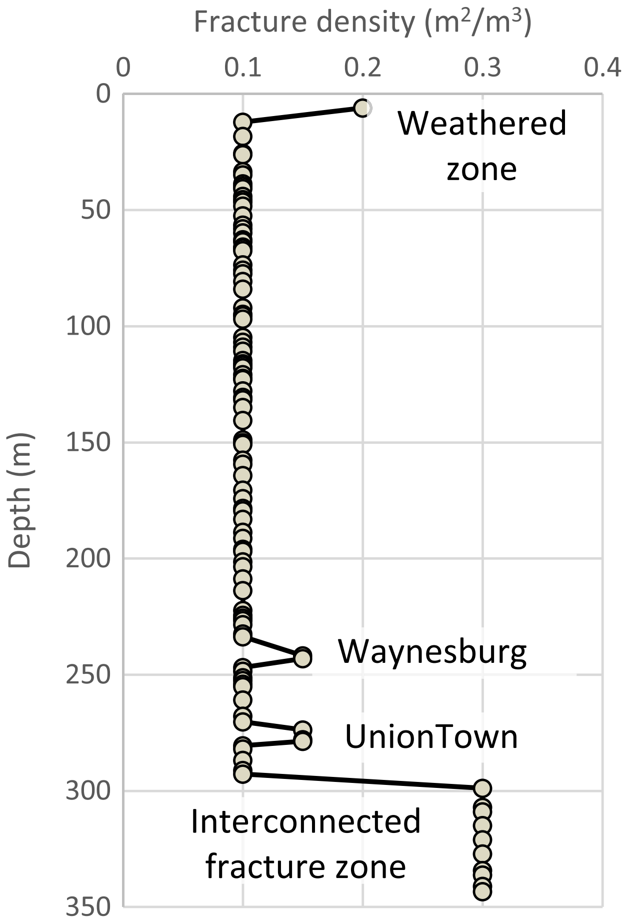

Fig. 3 DFN density applied to generate subvertical fractures

to the mine level. Through a set of field measurements, Palchik [8] suggested that the interconnected fracture zone is within 19–43 times the mining height and Khademian, et al. [4] showed this zone should probably be around 23 times the mining height. Thus, the interconnected fracture zone is considered 53-m thick. Khademian, et al. [4] also showed that the friction of both subvertical DFN fractures and bedding planes can be considered 60% of the internal friction of rock in each layer, except for the layers within the interconnected fracture zone with a constant friction angle of 10 degrees.

An initial value must be assigned for the aperture of the fractures in the model before applying the in situ stresses. Khademian et al. [4] showed that an initial aperture of 0.4–0.5 mm for both bedding planes and sub-vertical fractures, before applying in-situs tress in the model, gives a relatively good agreement between the pre-mining values of permeability from site measurements and models after applying the in situ stresses. So, the same initial apertures are assigned to the fractures in the model.

4.2 Gob model

The effects of gob materials on the mining-induced deformations due to the compaction of the gob and its residual voids are accounted for by installing a gob model at the roof of the panels. As indicated by [9], laboratory tests on shale and sandstone fragments showed that the stress-strain response of caved material should follow a strain-hardening curve. A hyperbolic function [10] in Eq. 1 was used to fit test results and was shown to sufficiently simulate the strain-hardening gob response.

$$\sigma = \frac{a \times \varepsilon}{b - \varepsilon} \quad (1)$$

In Eq. 1, σ is vertical gob stress (MPa), ε is vertical gob strain, b is maximum strain parameter related to the void ratio, and a is the gob stress where $\varepsilon = b/2$ (MPa). The laboratory tests showed that for shale gob: a = 7.7 MPa and b = 0.2 and for sandstone gob: a = 13 MPa and b = 0.3 [9].

Esterhuizen et al. [2] simulated the gob in FLAC3D with b=0.44 and a that ranged from 5.9 to 25.2 MPa, depending on the overburden type. They developed an equivalent element method where the caving zone is removed from the model and is replaced with zones whose cohesion is varied during the model run so that the gob stress follows the hyperbolic curve of Eq. 1. However, this approach in 3DEC may lead to excessive overlap of blocks within the equivalent element zones.

To avoid the excess overlap, the effects of the gob materials are simulated instead of explicitly modeling the caving process. To this end, after the panel is mined, counteracting loads are applied onto the mine roof in the model. The loads are gradually reduced until the mine roof is fully relaxed. The red dashed curve in Fig. 4 shows the average of the excavation-relaxing stresses applied onto the roof after mining the first panel in the model. At the same time, gob effects are modeled by applying incremental stresses at the same boundaries based on Eq. 1 with a vertical gob strain calculated as ε = roof displacement/caving height. With the assumption of b = 0.44 [2], the caving height is equal to 2.27 times the mining height because caved materials cannot be compacted to less than mining height. With a=5 MPa and b =0.44, reasonable gob response and maximum subsidence are obtained.

At every 1000th cycle, the gob strain was recorded, and the gob stress was applied onto the mine roof. The average of the gob-simulating stresses is shown as a solid black curve in Fig. 4.

At zero ro,of displacement in Fig. 4, the vertical stress applied onto the roof is the excavation-relaxing stress at 8.8 MPa (in-situ stress) and the gob stress is zero. As the excavation-relaxing stresses reduce to zero, the roof starts converging and thus giving rise to the gob-simulating stresses. The

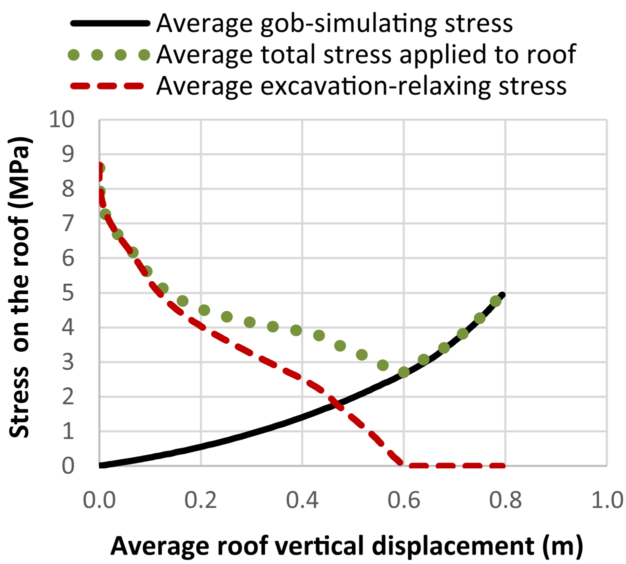

Fig. 4 Boundary loads applied to the mine roof in 3DEC model

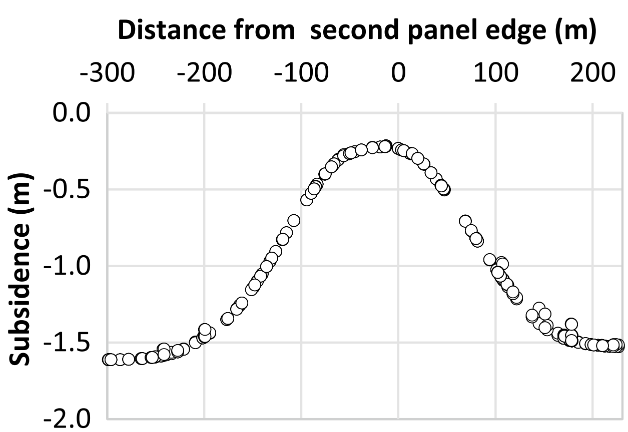

Fig. 5 Surface subsidence calculated in the 3DEC model with a maximum subsidence of 1.63 m

average of the resulting stresses on the roof is shown as a green-dotted curve in this figure, showing that the resulting stress follows the gob-simulating stress when the excavation-relaxing stress approaches zero. Once the model reaches equilibrium, the surface subsidence and pillar stresses are recorded. Figure 5 shows the super-critical surface subsidence recorded in the model with a maximum value of 1.63 m about 70% of the mining height that is expected from a supercritical longwall panel. Figure 6a and b show the modeled pillar vertical stress after the first and second panels are completed, respectively.

The in situ vertical stress at the mine level is about 9 MPa. After mining the first panel, the average vertical stress at the abutment pillar increases to 14 MPa. Mining the second panel increases the average vertical stress to 31 MPa. From the analysis of coal pillar stability (ACPS) calculation (Mark and Agioutantis, 2019), after mining the first panel, the stress is 17 MPa, and after the second panel mining, the stress reaches 43 MPa. Given the 3DEC model is two dimensional, as opposed to the ALPS calculation assumptions, the results are within the expected range of pillar stresses. Figure 6 also shows the gob stress after mining each panel. With the simulated gob effects, the stress within the roof gradually approaches the in situ stress level of 9 MPa, which reflects the expected gob effects after mining the panels.

4.3 Aperture variation

During mining of the two panels, apertures of all fractures are recorded in the model. Figure 7a and 7b show the aperture of the subvertical fractures and bedding planes, respectively. The aperture values in this figure correspond to the initial state of the model before loading in situ stresses, loaded state of the model, and after the first panel and second panel are completed. All fractures are initialized with an aperture width of 4 mm. In situ stresses expand the range of apertures from 4 mm to between 0.001 and 10 mm. This range further expands as mining continues in the panels with the second panel increasing the aperture of more fractures across the model.

Figure 7c compares the normalized frequency of aperture values in both subvertical fractures and bedding planes. Overall, bedding planes are associated with larger apertures with frequencies higher than that of the subvertical fractures. Due to the lack of field data on the fracture apertures, direct comparison with the in situ measurements is not an option. However, with the measured permeabilities from the slug tests in boreholes A and B, we can indirectly check the modeled apertures by comparing the modeled permeability with the measured values.

4.4 Permeability calculation

Permeabilities of subvertical fractures and bedding planes at each layer in the model are calculated and compared with measured values in borehole A and B in Figure 8. As discussed, rockmass permeability is mostly governed by the permeability of fractures; thus, we assume the rock matrix permeability is zero. The approach described in [4] based on the Cubic law and Darcy's equation is used for calculating the permeabilities in the model. For each layer from the ground surface down to the 341-m level, the permeability is calculated at three regions: an area within 10 m of distance to borehole A, an area within 10 m of distance to borehole B, and an area above the abutment pillar. The permeabilities in the first two regions allow comparison with the values measured from the slug test conducted in boreholes A and

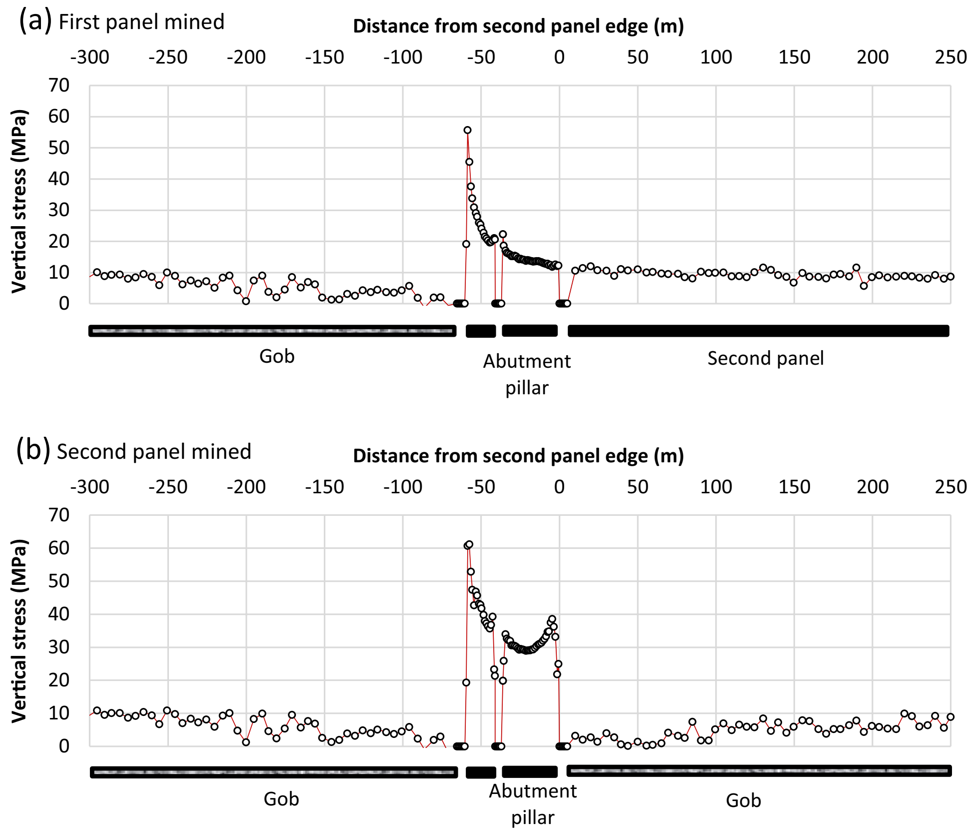

Fig. 6 Modeled pillar vertical stress (**a**) after mining the first panel and (**b**) after mining the second panel. The gob stress approaches the vertical in-situ stress, 9 MPa, at the mine level

B. The last region provides an understanding of permeability values around the potential gas well location. The 10 m of distance from the boreholes comes from the assumption that the slug test results represent permeability of rock within 10 m from the measurement points.

The red crosses in Fig. 8a and 8b show the field-measured values that sit between the modeled permeabilities of subvertical fractures and bedding planes, although closer to the subvertical fracture permeabilities. Note that the field slug test measures overall permeabilities that may be limited to the permeability of subvertical fractures or bedding planes or a combination of both, but there is no certain way of distinguishing the contribution of each group.

Figure 8c illustrates the modeled permeabilities above the abutment pillar showing that subvertical fracture permeabilities are in general less than the bedding plane permeabilities at shallow depths. This is because the ratio of the in situ horizontal stress to the vertical stress in the model is 3, typical of the Pittsburgh coal zone, and thus subvertical fracture apertures are smaller. When approaching to the mine level, the vertical stress induced by the longwall panel on the abutment pillar reduces the aperture values of bedding planes, and thus their permeabilities become closer to the subvertical fracture permeabilities. The relative agreement between the modeled and measured values of Fig. 8a and b and also the expected trend in Fig. 8c for permeability above the pillar allow for analyzing the gas flow through the fractured rock using the DFN geometry and modeled fracture apertures.

5 Inflow estimation

Once the fracture apertures are calculated in the geomechanical model, the range of potential inflow to the mining area can be calculated using Fracture Flow Code (FFC) [1]. The FFC generates a stochastic discrete fracture network for the study site using defined distributions. The fracture lengths are modeled with power distribution, and the location of the fractures are modeled using uniform distribution. The model utilizes a multi-zone approach to incorporate the exact aperture values from the geomechanical model to the FFC model.

An operating gas pressure head of 2.4 MPa (300 psi) is applied to the Sewickley horizon, 32 m above the mine roof. The pressure at the other locations is set to zero, except the mine roof, where a negative pressure is defined at the mine roof to represent the mine ventilation system. The shale gas is modeled as methane, and 100 DFN realizations are generated to represent multiple variations in the fracture geometry. The fractures are assumed to be 25% saturated with immobile water. Even though there

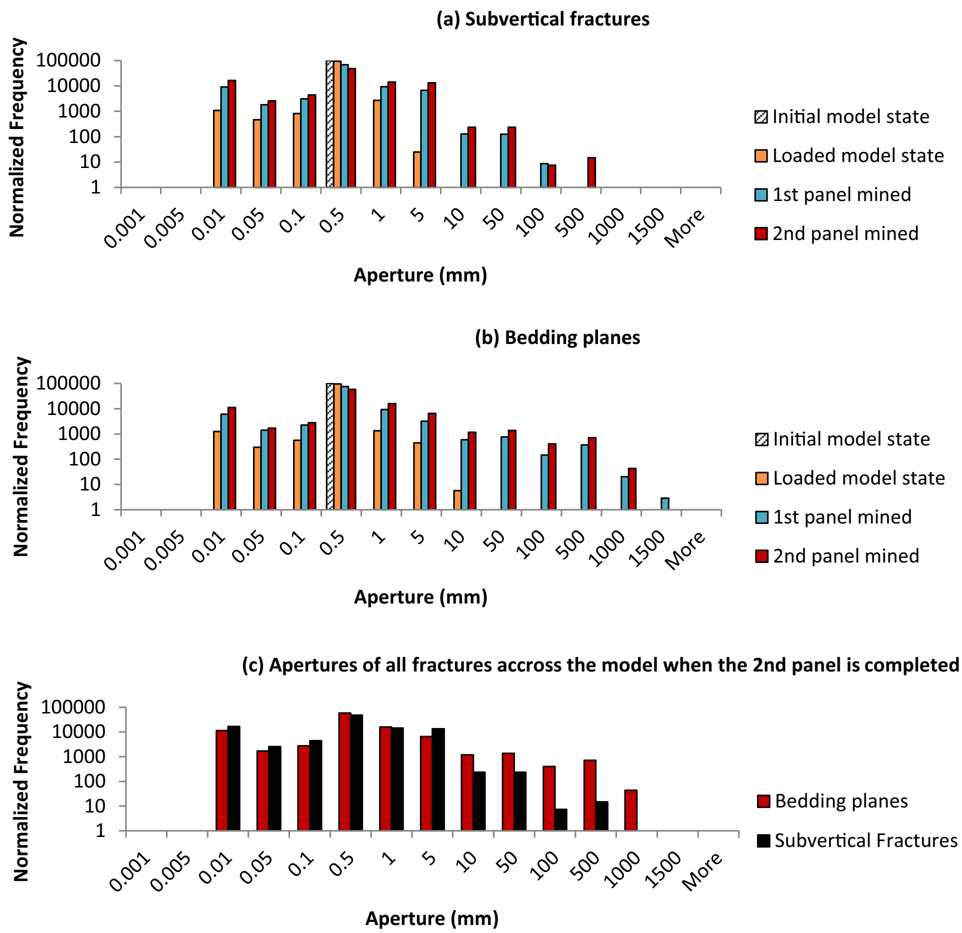

Fig. 7 3DEC results on the aperture values for (**a**) subvertical fractures and (**b**) bedding planes over the abutment pillar. (**c**) Comparison of bedding planes and subvertical fracture apertures after mining the second panel

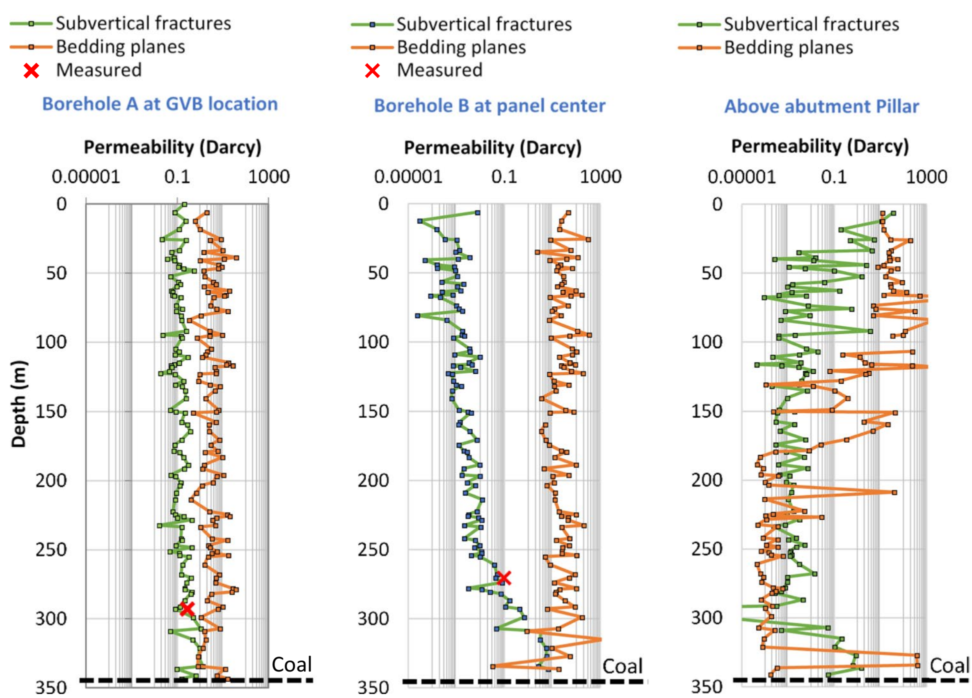

Fig. 8 Results of modeled and measured permeability by depth for when (**a**) first panel mining face is inby the test site at the GVB area in borehole A and (**b**) first panel mining face is outby the test site at the center of the first panel in borehole B. (c) The modeled permeabilities above the abutment pillar when second panel is outby the test site

could be several wells on a well pad, this study focuses on a single casing breach at the Sewickley horizon. One-hundred stochastic DFN realizations are generated to model variation in the fracture geometry, connectivity, and aperture.

The results show that the mean of the distribution is 0.006 m^3/s, which is significantly lower compared to the average of 0.22 m^3/s obtained from the data distribution for a hypothetical breach at the Sewickley horizon under the shallow-cover condition [4]. The significant differences between the potential gas flow for the deep and shallow site may be related to the difference in the mining-induced deformation and thus the permeability of the surrounding rockmass. However, detailed analyses will be performed in future studies to investigate the relationships between the rock permeability, depth of cover, and geology variations.

6 Discussion on limitations

It is important to note the limitations of the current methodology for estimating the permeability of fractures and calculating the potential inflow to the mine in the case of a gas well breach. Due to a lack of comprehensive field measurements, fracture geometries in the current model are borrowed from the previous calibration study on a shallower site with the overburden depth of 147 m, which can be a source of uncertainty. This is because the fracture geometries, such as the fracture density and orientation, can be site specific, depending on the depth of cover and mining layout along with the geology variation. Having said that, the geomechanical model under this assumption still reproduces the expected surface subsidence, pillar stress, and gob stresses. Also, the modeled permeabilities are shown to agree with two datapoints from field measurements. These observations along with previous validation efforts [4] help gain confidence on the accuracy of the approach and predicted aperture values, but further analyses are required to ensure the applicability of the developed methodologies for a wide range of mine layouts, overburden geology, and depths of cover.

In addition, the FFC is a 2D model with the assumption of a 1-m thickness in the out-of-plane direction; hence, the flow calculated is the total boundary flow per meter. This means the out-of-plane length for both the breached area (pressure source) and the fracture network is assumed to be 1 m. Changing this value, especially for the breached area, may change the results of the estimated inflow. Therefore, further investigation is needed to quantify the effects of the out-of-plane stress and deformation on the permeability of the surrounding rock and thus the potential inflow to the mine.

7 Conclusion

This paper uses a modeling methodology previously developed by researchers at NIOSH to investigate the rockmass permeability induced by mining the Pittsburgh coal seam under 341-m cover and estimates potential inflow to the mining area in case of a breached gas well in an abutment pillar. Surface subsidence, pillar stress, and gob material stresses are monitored in the pseudo-2D geomechanical model to ensure the results are within the expected range in similar mining conditions. The aperture of fractures across the model is calculated, and the results are checked against permeability measurements in two locations in the model. The aperture values are exported to the FFC model, and potential volumetric gas inflow to the mine is calculated for a hypothetical breach in the gas well located at the center of the abutment pillar. One hundred DFN realizations are simulated, and the results show that for a gas pressure of 2.4 MPa, the average of the inflow rates to the mine is 0.006 m^3/s, significantly lower than the average inflow of 0.22 m^3/s for a shallow cover mine studied in the previous work. Further analyses are needed to quantify the effects of geological parameters, mining layout, and overburden depth on the fracture aperture evolution and its effects on the inflow estimation. The quantified gas inflow ranges calculated in this paper will be used in ventilation network modeling tools for understanding the potential hazards of a shale gas well breach and evaluating the mitigation techniques.

Acknowledgements Data from this manuscript have been presented at the MINEXCHANGE 2022 SME Annual Conference & Expo, February 27–March 2, 2022, Salt Lake City, UT.

Declarations

Conflict of interest The authors declare no competing interests.

Disclaimer The findings and conclusions in this report are those of the author(s) and do not necessarily represent the official position of the National Institute for Occupational Safety and Health, Centers for Disease Control and Prevention (CDC). Mention of any company or product does not constitute endorsement by NIOSH.

References

1. Ajayi KM, Khademian Z, Schatzel SJ, Watkins E, & Gangrade V (2021) Numerical modeling of longwall-induced permeability under shallow cover. In Tukkaraja (Ed.), Mine Ventilation (pp. 389–397): CRC Press.
2. Esterhuizen GS, Mark C, and Murphy MM (2010) Numerical model calibration for simulating coal pillars, gob and overburden response. In proceeding of the 29th International Conference on Ground Control in Mining. Morgantown, WV: Barczak T, ed. 46–57

3. Feng G, Li Z, Hu S, Zhang Y, Zhang A, Gao Q, Cui J (2018) Distribution of gob empty space for methane drainage during the longwall mining: A case study. J Nat Gas Sci Eng 60:112–124. https://doi.org/10.1016/j.jngse.2018.09.026
4. Khademian Z, Ajayi KM, Su DWH, Esterhuizen G, and Schatzel SJ (2021) Geomechanical modeling of mining-induced permeability: implications for potential gas inflow from a sheared gas well. the 40th International Conference on Ground Control in Mining, Morgantown, WV.
5. Kohl WR (1980) Jointing in outcropping rocks of Pennsylvanian age, central Greater Pittsburgh region, Pennsylvania. U.S. Geological Survey, 80–23. https://doi.org/10.3133/ofr8023.
6. Mark C, Agioutantis Z (2019) Analysis of coal pillar stability (ACPS): a new generation of pillar design software. Int J Min Sci Technol 29:87–91
7. PADEP (2018). 2018 Oil and Gas Annual Report. Pennsylvania Department of Environmental Protection.
8. Palchik, V. (2003). Formation of fractured zones in overburden due to longwall mining. Environ Geol 44:(1) 28–38. https://doi.org/10.1007/s00254-002-0732-7
9. Pappas DM, and Mark C (1993). Behavior of Simulated Gob Material. U.S. Department of the Interior, Bureau of Mines, Report of Investigations 9458, 1993:1–39
10. Salamon MDG (1990). Mechanism of caving in longwall coal mining. Paper presented at the Rock Mechanics Contributions and Challenges: Proceedings of the 31st U.S. Symposium. https://doi.org/10.1201/9781003078944-26
11. Van Dyke MA, Zhang, P, Dougherty H, Su D, & Kim BH (2022) Identifying Longwall-Induced Fracture Zone Height Through Core Drilling. Mining, Metallurgy & Exploration. https://doi.org/10.1007/s42461-022-00622-z
12. Zhang P, Su D, Dougherty H, Kimutis R, Schatzel S, & Lu J (2020) A Case Study on Longwall Mining Near Shale Gas Wells in Barrier Pillars – Influence, Safety, and Risks. In the proceeding of the 54th U.S. Rock Mechanics/Geomechanics Symposium.
13. Zhang P, Dougherty H, Su DWH, Trackemas J, Tulu B (2020) Influence of longwall mining on the stability of gas wells in chain pillars. Int J Min Sci Technol 30(1):3–9